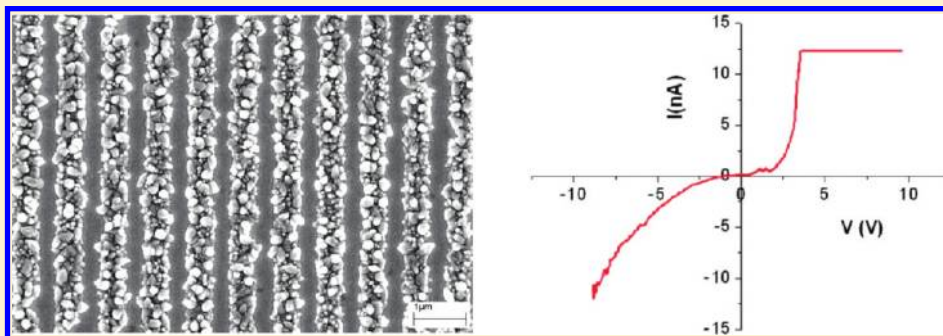


# Nanopatterning of Functional Materials by Gas Phase Pattern Deposition of Self-Assembled Molecular Thin Films in Combination with Electrodeposition

Antony George, A. Wouter Maijenburg, Minh Duc Nguyen, Michiel G. Maas, Dave H. A. Blank, and Johan E. ten Elshof\*

MESA<sup>+</sup> Institute for Nanotechnology, University of Twente, P.O. Box 217, 7500 AE Enschede, The Netherlands

## ABSTRACT:



We present a general methodology to pattern functional materials on the nanometer scale using self-assembled molecular templates on conducting substrates. A soft lithographic gas phase edge patterning process using poly(dimethylsiloxane) molds was employed to form electrically isolating organosilane patterns of a few nanometer thickness and a line width that could be tuned by varying the time of deposition. Electrodeposition was employed to deposit patterns of Ni and ZnO on these prepatterned substrates. Deposition occurred only on patches of the substrate where no organosilane monolayer was present. The process is simple, inexpensive, and scalable to large areas. We achieved formation of metallic and oxide material patterns with a lateral resolution of 80 nm.

## INTRODUCTION

Microcontact printing of alkanethiols<sup>1–3</sup> is the most studied method to pattern self-assembled monolayers (SAMs) on gold films. It has attracted wide research interest due to the ability of the patterned SAMs to act as etch resist<sup>1</sup> or as template for electrodeposition<sup>2</sup> or electroless deposition.<sup>3</sup> This makes patterned SAMs very important in future micro- and nanofabrication technologies. In microcontact printing, a soft poly(dimethylsiloxane) (PDMS) stamp inked with alkane thiol inks is pressed against a gold substrate to release the ink molecules in a controlled way to the substrate. The method is a scalable parallel process which is already implemented in industry to fabricate micrometer scale features. However, the miniaturization is still a challenge in microcontact printing due to the limitations of the elastomeric property of the PDMS stamp used and the limitation of ink diffusion<sup>4–7</sup> which may cause loss of fidelity and larger defect concentration of the patterns fabricated.

In order to minimize the defect concentration and overcome the problem of ink diffusion, it is necessary to develop new methodologies for patterning self-assembling molecules. Patterning a prefabricated film by area selective destruction or chemical modification by an electron beam<sup>8,9</sup> or AFM tip<sup>10–12</sup> are very efficient in terms of pattern fidelity and resolution. Prefabricated molecular films can have high film quality, since the

molecules are reacted from the liquid or gas phase for longer times when compared to short time microcontact printed films. Due to the serial nature and high capital investment costs of electron beam lithography and AFM lithography, these techniques can only be used in research. It is also possible to pattern high quality molecular thin films in a parallel manner using a preformed mask such as photoresist on a substrate, fabricated by photolithography<sup>13</sup> or nanoimprint lithography,<sup>14</sup> and followed by a gas phase or liquid phase deposition process of the self-assembling molecules and finally a resist removal step. However, these techniques require multiple process steps of resist patterning, etching, and/or residual layer removal.<sup>13,14</sup> Recently, we demonstrated a single step process for patterning organosilane SAMs from the gas phase using PDMS molds on silicon substrates.<sup>15</sup> The method can be employed to generate nanometer scale organosilane patterns using micrometer-sized PDMS molds due to the fact that organosilane molecules prefer to condense in geometrically restricted areas rather than condensing onto planar areas of the substrate. Patterns are therefore formed first at the three-phase boundary lines between substrate,

Received: June 12, 2011

Revised: August 26, 2011

Published: August 29, 2011

PDMS mold, and vapor, before condensing on geometrically planar patches. The lateral resolution of the formed patterns was about 1 order of magnitude smaller than the feature sizes of the PDMS mold.<sup>15</sup>

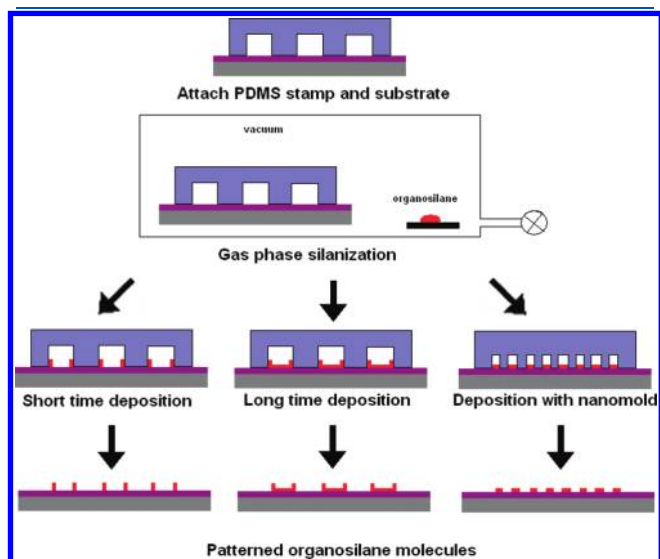


Figure 1. Schematic diagram of the patterning process.

In the present paper, we used the same patterning methodology to form mercaptosilane (MPTS) monolayers and thin films to act as patterned resists for subsequent fabrication of functional materials by electrodeposition. The process is a fast, inexpensive, and large area approach for pattern generation and can be employed in future device fabrication technologies. The schematic diagram of the process is described in Figure 1. A micro- or nanopatterned PDMS mold is pressed against a silicon substrate with a sputter deposited gold film of thickness  $\sim 75$  nm. A connected channel structure is formed between the mold and the substrate with openings to the ambient on the vertical side of the mold. The substrate–mold assembly is then exposed to a low pressure environment containing a source of self-assembling molecules for a certain period of time at a temperature of  $60$  °C. The natural vapor pressure of the mercaptosilane molecules at the given temperature leads eventually to the formation of a molecular thin film on the unshielded areas of the substrate. Depending on the time of exposure to vapor, two different modes of pattern generation are possible.<sup>15</sup> When the substrate is exposed to vapor for a limited period of time, patterns are formed only in the regions where the edges of the protruding regions of the PDMS mold are in contact. When the substrate is exposed for a longer period of time, the flat areas of the substrate are also covered by reactive mercaptosilane molecules. And as will be shown below, the difference between these two modes vanishes when the pattern resolution goes into the nanometer-scale domain. The three modes of patterning are shown schematically

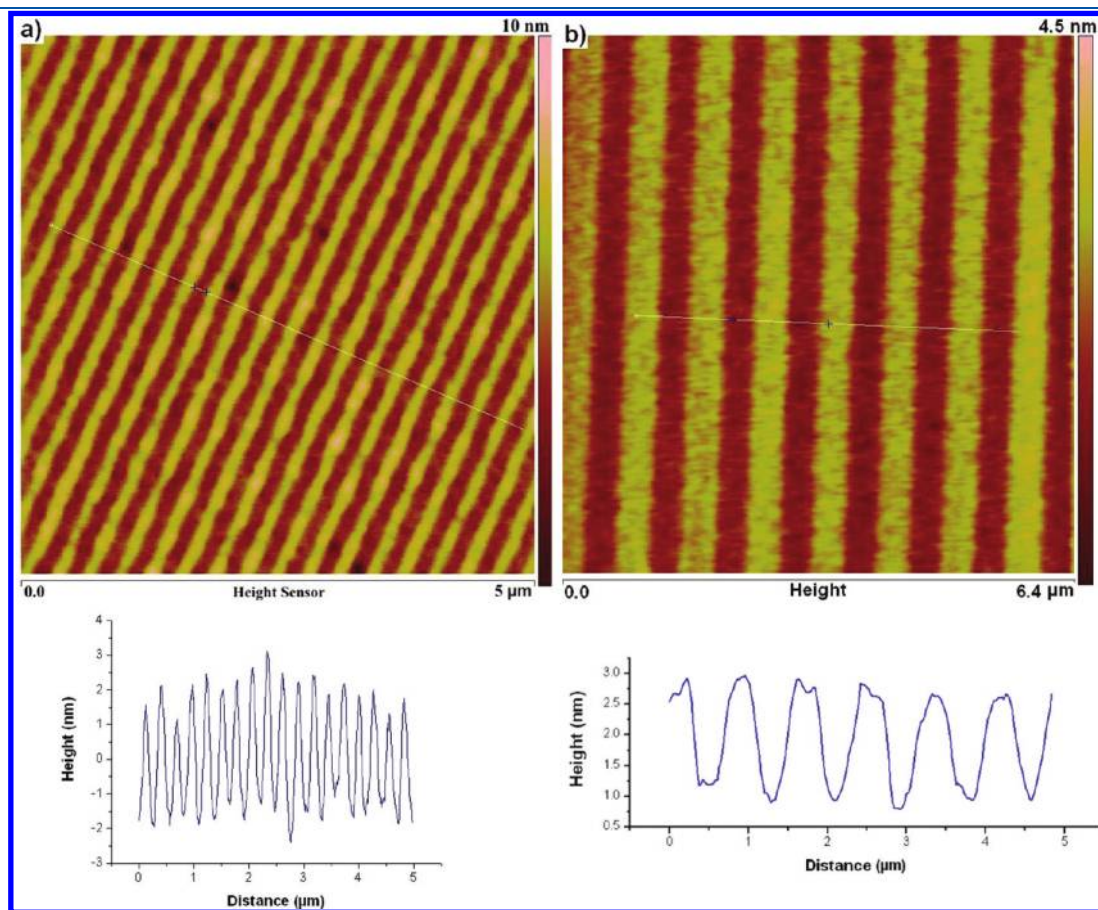
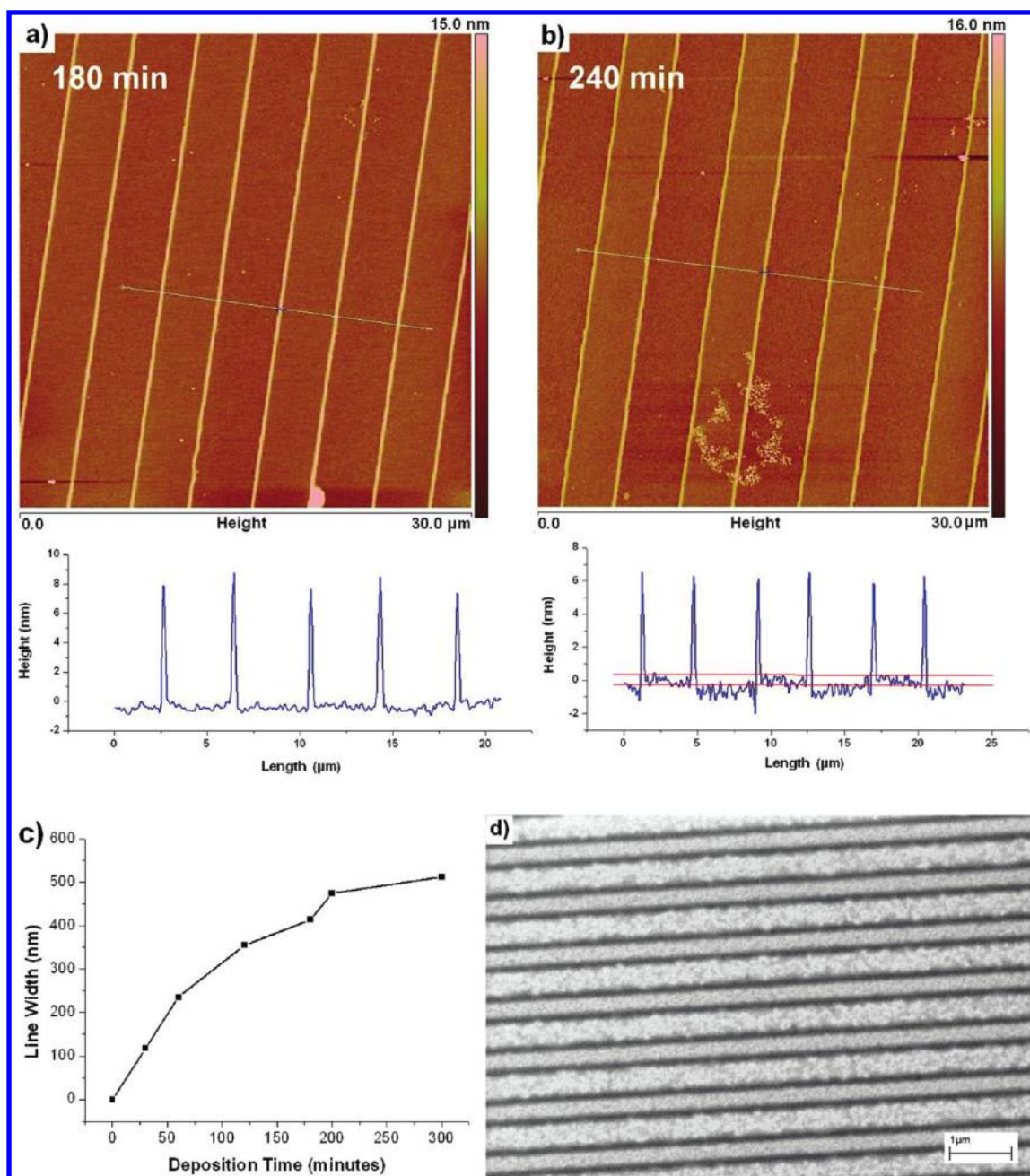


Figure 2. AFM image and AFM height profile of MPTS pattern. (a) Pattern with line width 110 nm, spacing 140 nm; (b) pattern with line width 350 nm, spacing 450 nm. Both patterns have a height of  $\sim 2$ – $3$  nm and were grown at  $60$  °C for 5 h.



**Figure 3.** Tapping mode AFM height images and AFM height profiles of MPTS lines formed (a) after 180 min of deposition and (b) after 240 min of deposition. The red lines in the height profile in (b) illustrate the height increase of  $>1$  nm of the planar area of the gold substrate. (c) Increase of width of edge-condensed lines with time. (d) HR-SEM image of condensed MPTS lines of 80 nm width on Au substrate, deposited using a PDMS mold of line width 350 nm, spacing 450 nm, and height 200 nm for 1 h at 60 °C.

in Figure 1. After organosilane deposition, the substrates were used as electrodes in an electrodeposition process to generate functional micropatterns of Ni and ZnO. We generated patterns with lateral resolutions ranging from  $\sim 80$  nm to a few micrometers.

## EXPERIMENTAL SECTION

**Fabrication of PDMS Molds.** PDMS and curing agent (Sylgard 184) were purchased from Dow Corning Corporation, mixed in a ratio 10:1, and poured over the micro/nanopatterned silicon master (created by photolithography or e-beam lithography). The PDMS was cured at a

temperature of 70 °C for 48 h. After curing, the PDMS molds were removed from the master and cut into pieces of  $1 \times 1$  cm<sup>2</sup> size.

**Preparation of Gold Coated Silicon Substrates.** p-Type silicon substrates cleaned with piranha solution (a mixture of H<sub>2</sub>O<sub>2</sub> and H<sub>2</sub>SO<sub>4</sub> in 1:3 volume ratio) were used in the experiments. The substrates were washed several times with deionized water and blow-dried in a nitrogen stream. Gold thin films of 75 nm thickness on silicon substrates were prepared using a Perkin-Elmer sputtering machine operating at 50 W at a deposition pressure of  $2 \times 10^{-5}$  mbar using argon as sputtering gas. A titanium film of thickness 10 nm was sputtered at 150 W as an adhesion promotion layer prior to gold sputtering.

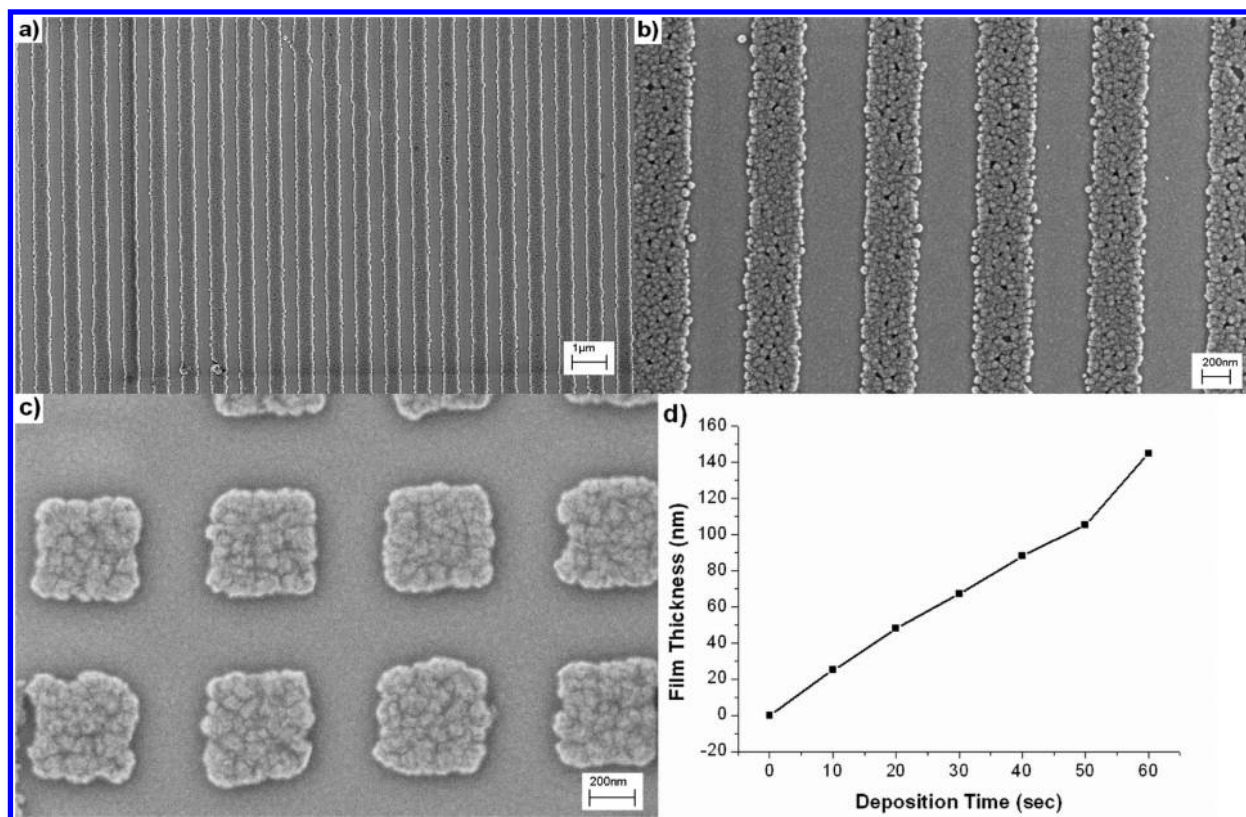


**Figure 4.** (a,b) Ni line patterns with width of  $\sim 350$  nm at two different magnifications. (c) Ni square patterns with a width of  $\sim 350$  nm. Patterns were grown for 30 s to  $\sim 60$  nm height. (d) Film thickness of Ni pattern by electrodeposition versus deposition time.

**Patterning Organosilanes.** (3-Mercaptopropyl)methyltrimethoxysilane (95% purity) (MPTS) was obtained from Sigma-Aldrich. The PDMS molds with micro/nanopatterned features were gently pressed against the gold coated silicon substrate. The patterned side of the mold faced the gold coated side of the silicon substrate. The PDMS mold made conformal contact with the substrate via van der Waals adhesion to the substrate. The PDMS can be peeled off the substrate easily by gentle force. The substrates with bonded PDMS mold were transferred to a desiccator. A drop of MPTS was placed in the desiccator and evacuated by a mechanical pump. The desiccator was heated to a temperature of  $60$  °C. A MPTS vapor saturated environment formed inside the desiccator. The organosilane molecules diffused from the gas phase into the PDMS channels and deposited on the substrates, forming covalent bonds with the Au surface. The substrates were exposed to the environment for a period of 1–12 h to study the effect of deposition time on pattern formation. After deposition, the substrates were taken from the desiccator and washed with absolute ethanol and deionized water and then stored for further analysis.

**Electrodeposition of ZnO and Ni.** MPTS patterned Au thin film substrates were used as substrate for electrodeposition. Electrodeposition was carried out using a three-electrode potentiostat (Autolab PGSTAT 128N, Metrohm Autolab B.V., The Netherlands). The SAM-patterned substrates were used as working electrodes. A small Pt mesh was used as counter electrode. The reference electrode was Ag/AgCl in 3 M KCl (Metrohm Autolab). Nickel patterns were formed from an electrolyte containing 0.23 M nickel sulfate hexahydrate ( $\text{NiSO}_4 \cdot 6\text{H}_2\text{O}$ , Sigma-Aldrich, purity 99%) and 0.15 M boric acid ( $\text{H}_3\text{BO}_3$ , Aldrich, purity 99.99%). Deposition occurred at  $-1.00$  V versus reference. Zinc oxide patterns were formed at  $60$  °C at  $-1.00$  V in an electrolyte containing 0.10 M zinc nitrate hexahydrate ( $\text{Zn}(\text{NO}_3)_2 \cdot 6\text{H}_2\text{O}$ , Sigma-Aldrich, purity 98%). Further details can be found elsewhere.<sup>16</sup>

**Characterization.** MPTS patterns were characterized using tapping mode atomic force microscopy (AFM; Veeco Dimension Icon) to determine the surface morphology. Tunneling current AFM (TUNA) was used to study the conductivity of the grown patterns as well as to map the conductivity of patterned surfaces.<sup>17</sup> Grown metal and oxide patterns were imaged using high resolution scanning electron microscopy (HR-SEM, Zeiss 1550) and tapping mode AFM. X-ray diffraction (XRD, Philips diffractometer PW 3020, Software XPert Data Collector 2.0e, Panalytical B.V., Almelo, The Netherlands) was used for phase determination of the patterns. The in-plane magnetic anisotropy of the polycrystalline Ni line arrays was characterized by using a vibrating sample magnetometer (VSM, model 10 VSM, Digital Measurement System 'DMS', ADE Technologies) at room temperature. Hysteresis loops were taken at different *in-plane* field directions with intervals of  $10^\circ$  field angle.

## RESULTS AND DISCUSSION

**Deposition of Organosilane Patterns.** Figure 2a shows a tapping mode AFM height image and AFM height profile of patterned mercaptosilane film on Au coated silicon substrate. The patterns were grown at a temperature of  $60$  °C for a period of 5 h. In principle, it should be possible to increase the rate of deposition further by working at higher vapor pressures, for example, by employing higher temperatures for deposition. The dimensions of the patterns in the PDMS molds are 110 nm line width, 140 nm spacing, and 100 nm channel height. A negative replica of the PDMS mold formed over the substrate with an approximate height of  $\sim 2$ – $3$  nm. Figure 2b shows an AFM image and AFM height profile of patterned mercaptosilane film on Au coated silicon substrate. The patterns were grown at a

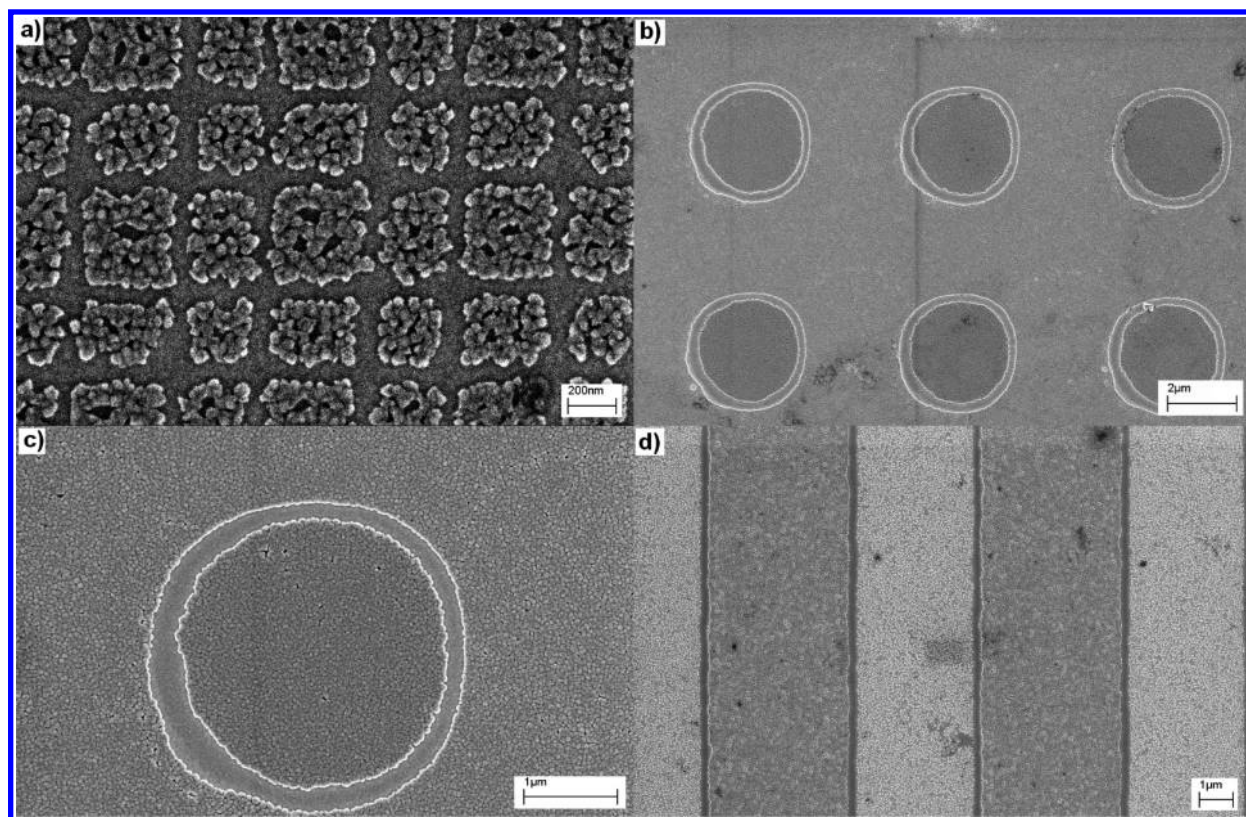


**Figure 5.** Nickel patterns on MPTS patterned Au substrates. (a) Square pattern (thickness 10 nm), MPTS line width  $\sim 80$  nm. (b,c) Inverse ring structure (thickness 120 nm), MPTS line width 350 nm. (d) Line patterns (thickness 120 nm) of  $\sim 4 \mu\text{m}$  width, MPTS line pattern had grown for  $\sim 12$  h.

temperature of  $60^\circ\text{C}$  for a period of 5 h. The dimensions of the patterns in the PDMS molds are 350 nm line width, 450 nm spacing, and 200 nm channel height. A negative replica of the MPTS mold formed over the substrate with an approximate height of  $\sim 2\text{--}3$  nm. The patterns were very homogeneous and of high quality. No difference could be observed between patterned areas near the outer edges of the PDMS mold and areas near the center of the mold.

We also used PDMS molds with micrometer and nanometer scale features for patterning MPTS thin films to exploit the possibility of preferable edge condensation of the organosilane molecules as we reported previously.<sup>15</sup> We grew MPTS patterns for different periods of time and studied the pattern formation process with a series of tapping mode AFM scans. Figure 3a,b shows tapping mode AFM images and height profiles of MPTS patterns grown for 180 and 240 min using a PDMS mold with a line pattern with lines of  $\sim 4 \mu\text{m}$  width and  $\sim 2 \mu\text{m}$  height grown at  $60^\circ\text{C}$ . The thick lines formed at the corners between the PDMS mold and the substrate indicate that MPTS molecules prefer to condense and polymerize initially in the corners rather than on the planar Au surface. The height of these edge patterns increased from  $\sim 1$  nm after 60 min to about 7–8 nm after 180–240 min. Further growth did not lead to a further increase of the height of the edge pattern. However, the AFM images also show an ongoing increase of the width of the edge patterns with time, as shown in Figure 3c. On the other hand, the unshielded planar areas of the Au substrate showed no signs of significant condensation of MPTS molecules during the first 180 min of deposition. Figure 3b shows an AFM image pattern after  $\sim 240$  min of growth. Here the uncovered planar areas between the corners

clearly increased height by  $<1$  nm. AFM scans of samples grown for 12 and 48 h (not shown here) showed that these areas did not increase thickness upon prolonged exposure to MPTS vapor. This indicates that, after the formation of about one monolayer, no further growth of the thickness of the SAM occurred. It is also possible to grow patterned MPTS films (up to 5–7 nm) by increasing the deposition temperature to  $70\text{--}80^\circ\text{C}$  for 3 h or more. An external load was applied to the PDMS mold to keep the mold on the substrate during the deposition process, since the PDMS molds were not stable and lifted off from the Au thin film (or lost conformal contact) above  $65^\circ\text{C}$ , probably due to expansion of the molds above this temperature.

Similar experiments with a nanometer scale patterned PDMS mold with a line width of 450 nm, an interline spacing of 350 nm, and a height of 200 nm also showed preferential condensation in the corners where PDMS and substrate meet during the first 2 h of deposition. After 1 h of deposition, the edge-condensed lines had a width of 80–90 nm as shown in the HR-SEM image of Figure 3d. However, due to the narrow size of the channels, a homogeneous MPTS film of 2–3 nm thickness formed across the width of the channels upon longer exposure. When we used a PDMS mold with a line width of 140 nm, a spacing of 110 nm, and a height of 100 nm (as shown in Figure 2a), we did not observe preferential corner condensation but only film formation across the entire surface of the channel.

By comparing the AFM images of MPTS patterns grown using microscale and nanoscale patterned PDMS molds, it can be concluded that the predominant mechanism of MPTS deposition in PDMS-substrate formed channels is geometry dominated

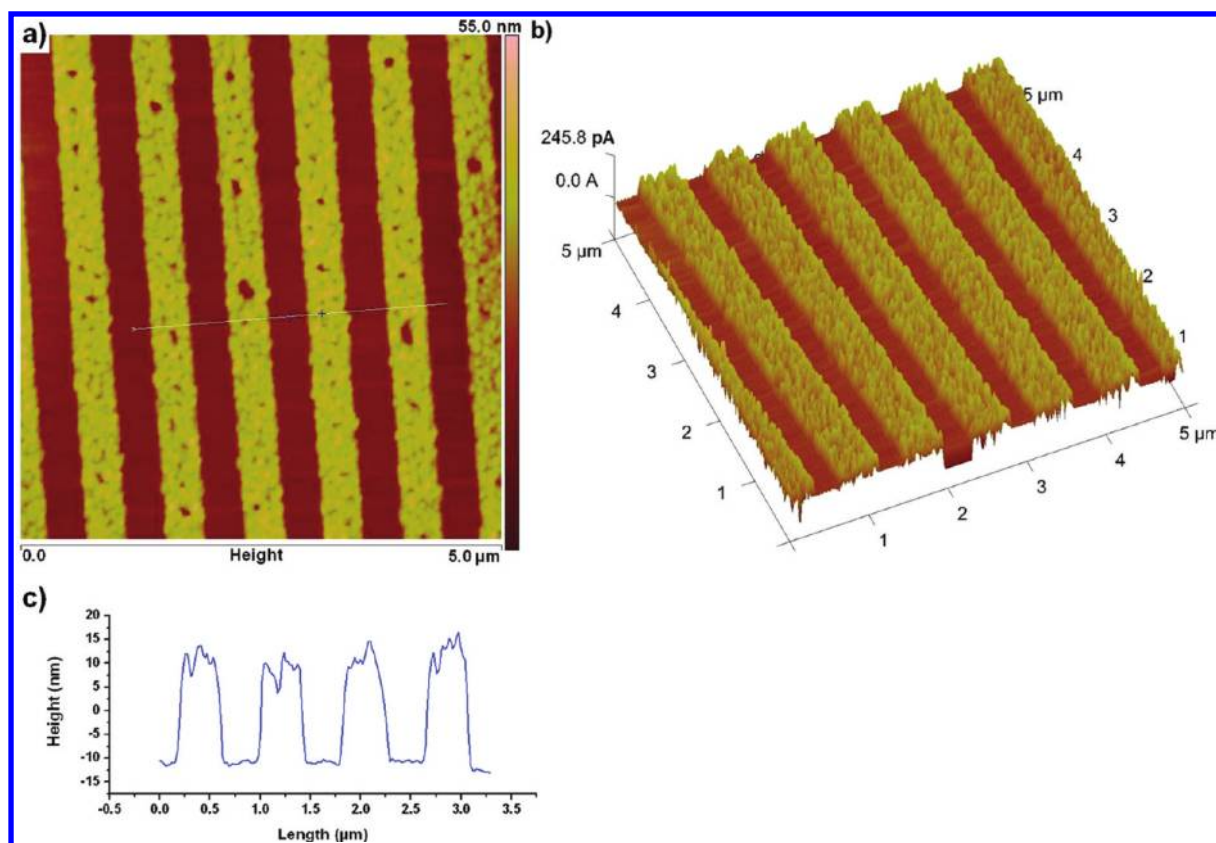


**Figure 6.** (a) AFM contact mode image of Ni pattern on MPTS-prepatterned Au substrate. (b) TUNA AFM conductivity map of Ni line pattern recorded at 1.121 mV applied sample bias versus AFM tip. (c) Contact mode height profile of the same pattern.

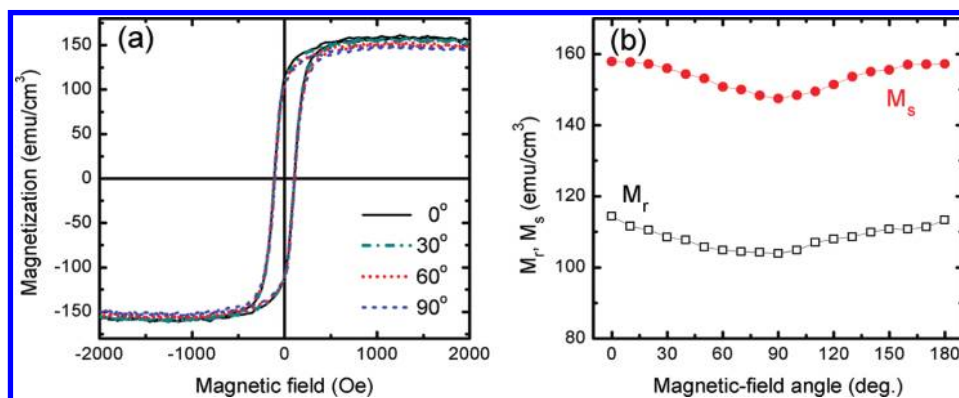


**Figure 7.** (a) Magnetic hysteresis ( $M-H$ ) loops and (b) remnant magnetization ( $M_r$ ) and saturation magnetization ( $M_s$ ) as a function of field angle of 80 nm thick Ni line arrays with a period of 800 nm and a line width of 450 nm on Au coated Si(100) substrate. The magnetic field was applied in-plane along a number of angles with respect to the direction of the lines.

adsorption/condensation of molecules in narrow corners by an effect similar to capillary condensation as described by Rascon and Perry.<sup>18</sup> Only in later stages of growth does complete coverage of the Au surface occur. When the channel dimensions go down to  $\sim 100$  nm or less, deposition by condensation occurs predominantly on the inside substrate surface.

**Electrodeposition Experiments.** The patterned MPTS thin films were used as templates to grow Ni and ZnO micro- and nanopatterns by electrodeposition. Ni was deposited on the uncovered parts of the MPTS patterned Au substrates using a bath containing nickel sulfate and boric acid at a potential of  $-1$  V.

Figure 4a–c shows HR-SEM images of Ni line and dot patterns. The Ni line width is  $\sim 350$  nm and has a spacing of 450 nm. The square dot patterns have a width of 350 nm, with a spacing of 450 nm between two dots. The patterns were deposited on an area of approximately  $1 \times 1$  cm<sup>2</sup>. We deposited Ni patterns for different periods of time, ranging from 5 s to 120 min. The Ni patterns could be grown up to  $\sim 200$  nm thickness without significant lateral growth. The rate of deposition was approximately 2 nm/s and was independent of deposition time. The grown Ni patterns were continuous and smooth irrespective of the deposition time. Longer deposition times ( $>2$  min) caused

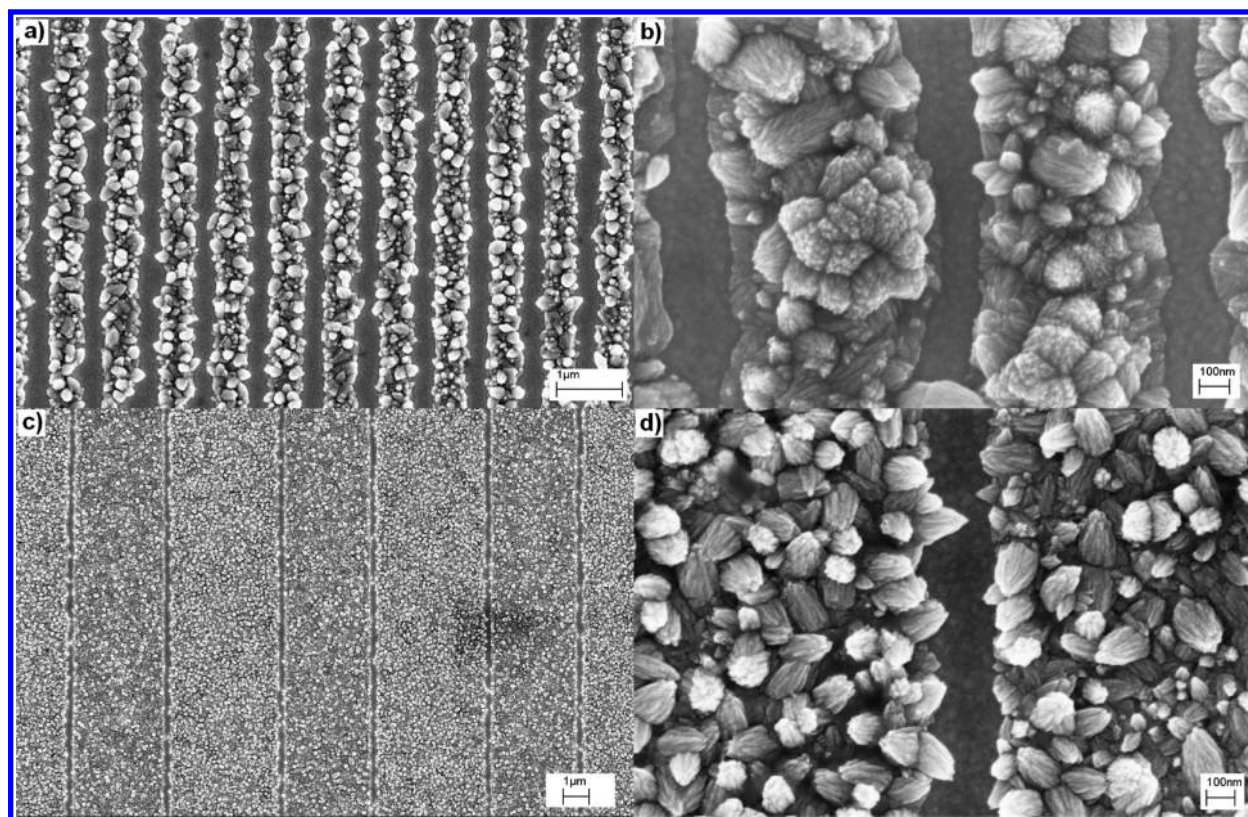


**Figure 8.** HR-SEM images of ZnO patterns on MPTS prepatterned Au thin film. (a) Line width  $\sim 450$  nm, spacing  $\sim 350$  nm; (b) line width 550 nm, spacing  $\sim 150$  nm. (c, d) ZnO lines grown on Au substrates with  $\sim 150$  nm wide MPTS line patterns.

lateral growth and resulted in widening of the lines. Figure 4d shows the Ni film thickness as function of deposition time.

Figure 5 shows Ni patterns grown on MPTS patterned Au substrates with edge-condensed  $\sim 80$  nm wide MPTS lines. Figure 5a shows 10 nm thick Ni nanopatterns by electrodeposition for 5 s on a substrate that was made using a nanometer-scale-patterned PDMS mold with a line width of 350 nm and a spacing of 450 nm. After the first deposition step, the mold was rotated by  $90^\circ$ , followed by a second deposition step under the same conditions to obtain a pattern of crossing lines. The spacing between all rectangular Ni dots was  $\sim 80$  nm, in agreement with the width of the patterned MPTS lines. Figure 5b and c shows Ni patterns grown for 1 min to obtain a thickness of  $\sim 120$  nm on Au substrates with ring-shaped MPTS patterns. The MPTS patterns had been grown for 3 h to a line width of  $\sim 350$  nm.

Figure 5d shows a Ni pattern electrodeposited on an MPTS line patterned substrate that had grown for 12 h. In this case, the MPTS film covered both corners and planar areas of the substrate. It is noted that the Ni film grew over the MPTS film. The SEM image shows that the density of the Ni film grown on the MPTS monolayer film was lower than the density of the film that had formed on bare patches of the electrode. It shows that the thin MPTS film is not completely isolating the substrate from electron transfer, which could be due to the low chain length of the molecules ( $>1$  nm) and/or small structural defects in the MPTS film. A film of MPTS with a height above  $\sim 1.5$  nm is completely isolating the substrate from electron transfer, as will be demonstrated below using TUNA conductivity mappings.

The conductivity of the Ni patterns was characterized via tunneling AFM (TUNA). Figure 6 shows the contact mode AFM

image, TUNA conductivity map, and contact mode height profile of Ni line patterns with a nominal thickness of 20 nm (10 s of deposition time). The contact mode image and conductivity map were recorded simultaneously with an applied sample bias of 1.221 mV versus the AFM tip. The data illustrate the uniform high conductivity of the Ni patterns.

Figure 7a shows the  $M-H$  loops at room temperature at directions  $0^\circ$ ,  $30^\circ$ ,  $60^\circ$ , and  $90^\circ$  with respect to the edge of the substrate. As can be seen in Figure 7b, both  $M_r$  and  $M_s$  oscillate with a periodicity of  $180^\circ$ , with the highest value at  $0^\circ$  and the lowest value at  $90^\circ$ . The highest values of  $M_r$  and  $M_s$  are 115 and 158  $\text{emu}/\text{cm}^3$ , respectively.

The saturation magnetization is smaller than that of bulk Ni ( $484 \text{ emu}/\text{cm}^3$ ).<sup>19</sup> However, the values did not change much with the change of field angle. This indicates that the films have a weak in-plane magnetic anisotropy. Regarding the origin of magnetic anisotropy in the films, we consider two main sources of the magnetic anisotropy: magnetic dipolar interaction (shape anisotropy) and spin-orbit interactions (magnetocrystalline anisotropy and magneto-elastic anisotropy), as outlined in detail in ref 20. As can be seen in the  $M-H$  loops, the  $M_r$  value was much smaller than the  $M_s$  value at any filed angle, and the easy axis could not be determined easily. So the magnetocrystalline anisotropy is not dominant, and this points to the polycrystalline nature of the electrodeposited Ni patterns. The  $M_r$  and  $M_s$  values were probably affected by shape anisotropy normally observed in polycrystalline materials.

ZnO patterns were grown from an aqueous zinc nitrate electrolyte solution at a voltage of  $-1$  V versus reference. Figure 8a shows ZnO patterns that were deposited on a MPTS

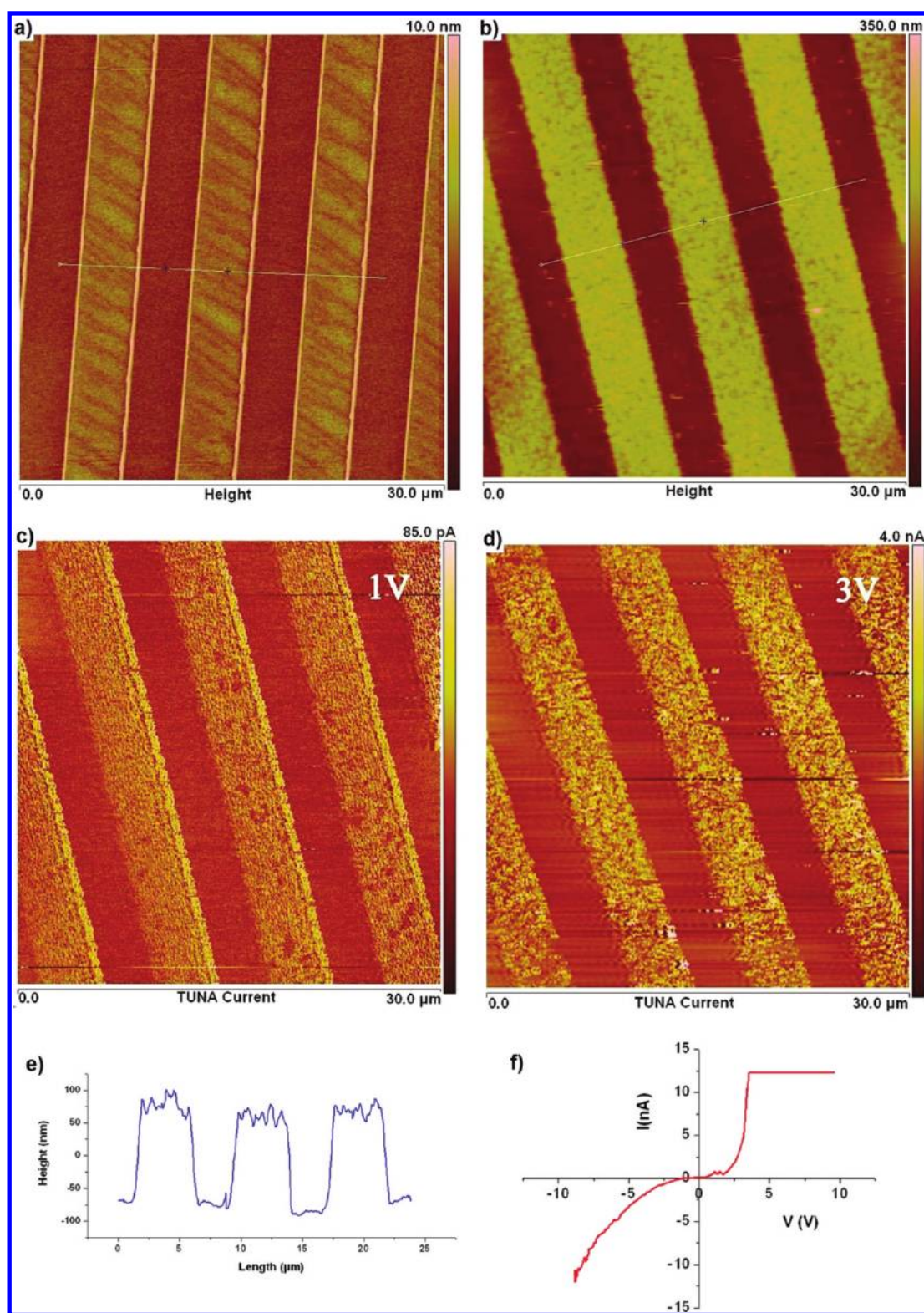


**Figure 9.** (a) Tapping mode AFM image of patterned MPTS thin film grown at 70 °C for 2 h. (b) Contact mode AFM image of ZnO line pattern electrodeposited on MPTS thin film as shown in (a). (c) TUNA conductivity of ZnO line patterns at applied sample bias of 1 V with respect to AFM tip. (d) TUNA conductivity of ZnO line patterns at applied sample bias of 3 V with respect to AFM tip. (e) Contact mode AFM height profile of ZnO pattern. (f) TUNA  $I$ – $V$  characteristics of electrodeposited ZnO.

line-patterned substrate with  $\sim 400$  nm line width. The ZnO patterns have a line width of 450 nm and a spacing of 350 nm. Figure 8b shows  $\sim 600$  nm wide patterned ZnO lines with a gap

of  $\sim 150$  nm between them. The gap was formed using edge condensation of MPTS for  $\sim 90$  min using a PDMS mold with a line width of 600 nm and a spacing of 800 nm. Figure 8c,d shows

a ZnO line pattern grown on a MPTS prepatterned gold substrate. The MPTS lines had been deposited for 60 min, and condensation had occurred preferentially in the corners. The lines had a width of  $\sim 160$  nm. After ZnO electrodeposition, a spacing of  $\sim 140$  nm was present between the  $\sim 4$   $\mu\text{m}$  wide ZnO lines.

The conductivity of ZnO patterns was also characterized via tunneling AFM (TUNA). Figure 9a shows a tapping mode AFM image of a MPTS film formed using a PDMS mold with a line width and spacing of  $\sim 4$   $\mu\text{m}$ . The MPTS thin film was grown for 2 h at  $70$   $^{\circ}\text{C}$  to a thickness of  $\sim 1.5$  nm. A small load was placed on the PDMS mold to keep it in conformal contact with the substrate at this temperature. Figure 9b–e shows the contact mode AFM image, TUNA conductivity map recorded at a sample bias of 1 V versus AFM tip, TUNA conductivity map recorded at a sample bias of 3 V versus AFM tip, and an AFM height profile of the ZnO line patterns grown by electrodeposition on MPTS patterned Au substrate as shown in Figure 9a. The data in Figure 9b, c, and e were recorded simultaneously with an applied sample bias of 1 V versus the AFM tip. The data show uniform conductivity of the ZnO patterns. The relatively low tunneling currents at both applied voltages show the semiconducting nature of ZnO line pattern. In this case, the MPTS-covered patches of the substrates showed no conductivity at applied voltages up to at least 5 V, which illustrates the high electrical resistance of MPTS thin films of  $\sim 1.5$ –2 nm thickness. This is very important when they are to be used as resists in electrodeposition processes. Figure 9f shows TUNA  $I$ – $V$  characteristics of electrodeposited ZnO measured at a particular position in a patterned line. The shape of the  $I$ – $V$  curve is characteristic of semiconducting materials and illustrates the semiconducting behavior of the ZnO patterns. In order to obtain consistent data, the  $I$ – $V$  characteristics were recorded at several points of the patterned lines.

## CONCLUSIONS

We presented an easy and cost-effective methodology to pattern mercaptosilane thin films on the nanoscale using micro- and nanometer-scale PDMS molds. We observed preferable condensation of mercaptosilane molecules in the corners where the vertical wall of the PDMS channel came in contact with the gold substrate during the initial stages of the deposition process, so that very thin lines of MPTS with a width of 80 nm could be established when the deposition time of MPTS was kept limited. After prolonged periods of MPTS deposition, we also observed a thin mercaptosilane layer on all unshielded areas of the substrate, but no film thickness increase was observed when the time of exposure was increased further. When nanometer-scale molds were used, the MPTS molecules condensed directly across the width of the channels, due to its small dimensions. The method can be used to pattern mercaptosilane lines down to a lateral dimension of 80 nm on gold substrates. We used mercaptosilane patterns as templates for electrodeposition of Ni and ZnO. The method can be employed to deposit a wide range of functional material patterns that can have potential applications in the fabrication of functional devices. The process is easily upscalable provided that the mold is carefully designed to minimize the diffusion length of condensable vapor inside the channels of the substrate–mold assembly.

## AUTHOR INFORMATION

### Corresponding Author

\*E-mail: j.e.tenelshof@utwente.nl

## ACKNOWLEDGMENT

Financial support of NWO-STW in the framework of the Vernieuwingsimpuls programme (VIDI) is acknowledged.

## REFERENCES

- (1) Kumar, A.; Whitesides, G. M. *Appl. Phys. Lett.* **1993**, *63*, 2002–2004.
- (2) Pesika, N. S.; Radisic, A.; Stebe, K. J.; Searson, P. C. *Nano Lett.* **2006**, *6*, 1023–1026.
- (3) Hsu, C.-H.; Yeh, M.-C.; Lo, K.-L.; Chen, L.-J. *Langmuir* **2007**, *23*, 12111–12118.
- (4) Jeon, N. L.; Finnie, K.; Branshaw, K.; Nuzzo, R. G. *Langmuir* **1997**, *13*, 3382–3391.
- (5) Biebuyck, H. A.; Larsen, N. B.; Delamarche, E.; Michel, B. *IBM J. Res. Dev.* **1997**, *41*, 159–170.
- (6) Delamarche, E.; Schmid, H.; Bietsch, A.; Larsen, N. B.; Rothuizen, H.; Michel, B.; Biebuyck, H. *J. Phys. Chem. B* **1998**, *102*, 3324–3334.
- (7) Dameron, A. A.; Hampton, J. R.; Smith, R. K.; Mullen, T. J.; Gillmor, S. D.; Weiss, P. S. *Nano Lett.* **2005**, *5*, 1834–1837.
- (8) Zhang, G.-J.; Tani, T.; Zako, T.; Hosaka, T.; Miyake, T.; Kanari, Y.; Funatsu, T.; Ohdomari, I. *Small* **2005**, *1*, 833–837.
- (9) Pallandre, A.; Glinel, K.; Jonas, A. M.; Nysten, B. *Nano Lett.* **2004**, *4*, 365–371.
- (10) Maoz, R.; Frydman, E.; Cohen, S. R.; Sagiv, J. *Adv. Mater.* **2000**, *12*, 725.
- (11) Rosa, L. G.; Jiang, J. Y.; Lima, O. V.; Xiao, J.; Utreras, E.; Dowben, P. A.; Tan, L. *Mater. Lett.* **2009**, *63*, 961–964.
- (12) Seo, K.; Borguet, E. *Langmuir* **2006**, *22*, 1388–1391.
- (13) Anderson, M. E.; Srinivasan, C.; Hohman, J. N.; Carter, E. M.; Horn, M. W.; Weiss, P. S. *Adv. Mater.* **2006**, *18*, 3258–3260.
- (14) Maury, P.; Péter, M.; Mahalingam, V.; Reinhoudt, D. N.; Huskens, J. *Adv. Funct. Mater.* **2005**, *15*, 451–457.
- (15) George, A.; Blank, D. H. A.; ten Elshof, J. E. *Langmuir* **2009**, *25*, 13298–13301.
- (16) Maas, M. G.; Rodijk, E. J. B.; Maijenburg, A. W.; Blank, D. H. A.; Ten Elshof, J. E., *J. Mater. Res.* **2011**, DOI: 10.1557/jmr.2011.93.
- (17) Veeco AFM Manual, Application Modules, Nanoscope V7-B (004-1020-000).
- (18) Rascon, C.; Parry, A. O. *Nature* **2000**, *407*, 986–989.
- (19) Chow, G. M.; Zhang, J.; Li, Y. Y.; Ding, J.; Goh, W. C. *Mater. Sci. Eng., A* **2001**, *304*–306, 194–199.
- (20) Johnson, M. T.; Bloemen, P. J. H.; denBroeder, F. J. A.; deVries, J. J. *Rep. Prog. Phys.* **1996**, *59*, 1409–1458.